Copy 6
RM E55L09

NACA RM E55L09

NACA

RESEARCH MEMORANDUM

EXPERIMENTAL INVESTIGATION OF A 0.4 HUB-TIP DIAMETER RATIO AXIAL-FLOW COMPRESSOR INLET STAGE AT TRANSONIC INLET RELATIVE MACH NUMBERS III - EFFECT OF TIP TAPER ON OVER-ALL AND BLADE-ELEMENT PERFORMANCES

By John C. Montgomery and Frederick Glaser

Lewis Flight Propulsion Laboratory
Cleveland, Ohio

NATIONAL ADVISORY COMMITTEE
FOR AERONAUTICS

WASHINGTON

March 30, 1956

NATIONAL ADVISORY COMMITTEE FOR AERONAUTICS

RESEARCH MEMORANDUM

EXPERIMENTAL INVESTIGATION OF A 0.4 HUB-TIP DIAMETER RATIO AXIAL-FLOW COMPRESSOR INLET STAGE AT TRANSONIC INLET RELATIVE MACH NUMBERS

III - EFFECT OF TIP TAPER ON OVER-ALL AND BLADE-ELEMENT PERFORMANCES

By John C. Montgomery and Frederick Glaser

SUMMARY

An investigation was conducted to determine the feasibility of increasing the tip-section blade-element efficiency of a transonic rotor by reducing the blade loading for a given design inlet relative Mach number. The 0.4 hub-tip diameter ratio transonic rotor was modified by tapering the outer casing inward across the rotor-blade row. The blades were unchanged except that the tips were machined down to fit the new outer-casing contour. The reduced outlet area and the streamline curvature thus obtained increased the outlet tip axial velocity and decreased the tip-section blade loading for a given inlet relative Mach number.

At the design corrected tip speed of 1000 feet per second, the rotor modification increased the over-all-performance peak efficiency from 0.93 to 0.95 and decreased the maximum pressure ratio from 1.42 to 1.40. A larger useful weight-flow range was obtained for the modified rotor at design speed. At 115 percent design speed, the over-all-performance peak efficiency for the rotor modification was 0.92.

At design speed, the rotor modification increased the tip-section blade-element peak efficiency from 0.80 to 0.92. The rotor modification also decreased the diffusion factor at the near-minimum-loss incidence angle of 4.5° at the tip section from 0.45 to 0.30. For a given diffusion-factor value of 0.40, the rotor modification decreased the total-pressure-loss coefficient at the rotor tip section from 0.14 to 0.075.

Curvature on the outer casing had a pronounced effect on the rotor inlet and outlet axial-velocity distributions, and this effect should be included in obtaining velocity diagrams for designs which incorporate tip curvature.

INTRODUCTION

The investigation of the over-all performance of a 0.4 hub-tip diameter ratio transonic rotor designed to handle 34.9 pounds of air per second per square foot of rotor frontal area (ref. 1) has indicated that a rotor average efficiency of approximately 0.90 could be obtained with high flow capacity. A more detailed analysis of the performance of each blade element of this rotor (ref. 2) indicated that the efficiency of the rotor-blade tip section decreased markedly as the speed was increased to the design speed. It is pointed out in reference 2 that this drop in tip efficiency with increase in speed was probably the result of the increased blade loading (as defined by the diffusion factor of ref. 3 and the axial-velocity reduction across the tip section) rather than the result of shock losses caused by the increase in the Mach number relative to the rotor blade. Decreased tip-section blade-element efficiencies at design speed were also experienced for the transonic rotors of references 4 to 6.

It was felt that a separation of the effects of blade loading and Mach number would be desirable in order to give a more conclusive explanation for the decrease in tip efficiency with increase in rotor speed. A simple technique for separation of these effects was, therefore, derived. The original rotor was modified by inserting a spacer and tapering the outer casing inward across the rotor-blade row so as to reduce the area of the rotor outlet. The rotor blades were unchanged except that the tips were machined down to fit the altered outer-casing contour. The taper across the rotor was made nonlinear so that the outer casing had a convex curvature. Since the outer casing was not altered upstream of the rotor-blade leading edge, the inlet geometry of the compressor was unchanged.

The effect of the reduced area at the rotor outlet and the streamline curvature introduced by the curvature (nonlinear taper) of the outer casing was to increase the axial velocity leaving the rotor for any given inlet Mach number. The effect of the increase in axial velocity was, in turn, to decrease the diffusion factor at the rotor tip section for a given relative inlet Mach number.

The tip section of the modified rotor was taken, as in the case of the original rotor, as that section 10 percent of the passage height from the outer wall. Therefore, the geometry of the modified rotor-blade tip section is not identical to the geometry of the tip section of the original rotor.

The difference in blade geometry (camber, thickness, and chord) between the two rotor-blade tip sections is slight, and the effect of these changes is considered small as compared with the change in blade loading.

The present report discusses the over-all and blade-element performances of the modified rotor and compares them with the performance of the original rotor. A discussion of the effects of the streamline curvature introduced by the nonlinear taper of the outer casing on the velocity distributions through the annular flow area is also presented.

APPARATUS AND PROCEDURE

Rotor Design and Modification

The rotor design is presented in detail in reference 1. The rotor was designed to produce a total-pressure ratio of 1.35 at a specific corrected weight flow of 34.9 pounds per second per square foot of frontal area and a tip speed of 1000 feet per second. The diameter of the rotor was 14 inches, and the inlet hub-tip diameter ratio was 0.4. The rotor was designed for axial air inlet and constant energy addition along the radius.

For the modified rotor, the outer-casing contour was altered by means of an insert located along the outer casing, as shown in figure 1. The tip insert had a circular-arc taper of 4.5-inch radius, with the insert thickness increasing from zero at the rotor leading edge to a maximum value of 0.25 inch at the rotor outlet. With the effect of the streamline curvature due to the new outer-casing contour on the radial distribution of velocity neglected, the thickness of the insert was selected as that value required to increase the axial-velocity ratio across the rotor at design speed approximately 10 percent (from 0.92 for the untapered rotor tip section to 1.02 for the tapered rotor tip section). Because of the positive radius of curvature of the insert, the effect of streamline curvature would be an increase in the axial-velocity ratio $V_{z,2}/V_{z,1}$ across the rotor tip to a value somewhat greater than the predicted 10-percent increase based on area change alone. The small radius of 4.5 inches was selected rather arbitrarily so as to accentuate the effects of streamline curvature in giving a large increase in axial-velocity ratio for this investigation.

The modified rotor was tested with the altered hub contour shown in figure 1. This alteration of the hub section had been made previously with the original rotor for the purpose of reducing the loss through the hub section of the stator blades. As reported in reference 2, the altered outlet hub section had a negligible effect on the stator-blade-element performance.

The tip section of both the original and modified rotors was taken as that blade section 10 percent of the passage height from the outer wall. Therefore, the designated blade tip sections for the two rotors varied, as shown in figure 1. The contour of the two rotor-blade tip

sections is shown in figure 2. The variation in chord length between the two blade sections is negligible, but the blade camber angle was increased from 11.4° for the untapered rotor to 14.6° for the modified or tapered rotor. The blade tip-section contours shown in figure 2 are copies of prints made 20 times the actual size of the blade contour taken along the two tip sections, as shown in figure 1. The variation of the blade camber angles and the outlet-measuring-station radius ratios for the original and modified rotors are presented in table I.

In order to minimize or eliminate the effect of variations of tip clearance in this investigation, the tip clearance was maintained at the same value (0.025 to 0.028 in.) used for the original rotor investigation.

3698

Compressor Installation and Instrumentation

The compressor installation and instrumentation are the same as those described in reference 2 except that (1) measurements after the rotor were recorded continually by an automatic recorder as each instrument was traversed radially across the rotor passage height, and (2) the facilities of the test unit were altered during the test program so that refrigerated air (down to -60° F) could be supplied to the compressor inlet.

The facilities for supplying refrigerated air to the compressor inlet were not installed until after the modified rotor was tested at corrected tip speeds of 600, 800, 1000, and 1050 feet per second. The installation of the refrigerated air system enabled the overspeed run of 115 percent of design speed (or a tip speed of 1150 ft/sec) to be made without increasing the actual mechanical speed of the rotor above the value previously used at 105 percent design speed.

The weight flow indicated by the new orifice used for the runs at 115 percent design speed was approximately 2-percent less than the weight flow indicated by the original inlet orifice. Therefore, in order to present a consistent over-all compressor performance map, the weight flows measured by the new orifice (115-percent-design-speed runs) were corrected to that value which would have been measured by the original orifice.

A plug-type vibration pickup mounted in the casing over the rotor was used to indicate blade vibrations. The plug-type vibration pickup is a magnetic-type unit which generates a voltage proportional to the velocity of the rotating blade. The plug-type pickup is used in conjunction with an oscilloscope to produce a continuous pattern which is proportional to the blade speed. When blade vibration occurs, the voltage output of the pickup plug is increased for the fixed rotational speed, and this increased voltage (increased blade velocity) is indicated on the oscilloscope pattern.

[redacted]

Procedure

Data for the modified rotor were taken at corrected speeds of 60, 80, 100, 105, and 115 percent of design speed. At each speed the weight flow was varied over the complete vibration-free weight-flow range. The over-all performance of the rotor is presented as arithmetically averaged values so as to be consistent with the data presented in references 1 and 2.

The symbols and equations used in computing the blade-element and over-all performance are included in appendixes A and B, respectively. A typical velocity diagram illustrating the air and blade angles is given in figure 3.

COMPARISON OF ORIGINAL AND MODIFIED ROTOR PERFORMANCES

Over-All Performance

The over-all performance of the modified rotor is compared with the over-all performance of the original rotor (ref. 2) in figure 4 for corrected tip speeds of 600, 800, 1000, 1050, and 1150 feet per second. At a corrected tip speed of 1150 feet per second, data are presented only for the modified rotor because refrigerated air was not available for the tests of the original rotor configuration. The overspeed data of 1150 feet per second are presented as dashed curves in order to indicate that the weight flow was corrected to the value which would have been indicated by the original inlet measuring orifice.

For the modified rotor, the design-speed total-pressure ratio of 1.35 (the design value for the original rotor) was obtained at a corrected specific weight flow of 33.7 pounds per second per square foot of frontal area and at an adiabatic efficiency of 0.95. The peak efficiency at design speed was also 0.95. Peak efficiencies of 0.94, 0.95, and 0.94 were obtained at 60, 80, and 105 percent design speed, respectively. For the refrigerated overspeed run of 1150 feet per second, a peak efficiency of 0.92 was obtained.

The effect of the rotor modification (fig. 4) was to decrease the specific weight flow from 34.4 to 33.7 pounds per second per square foot of frontal area at design speed and a total-pressure ratio of 1.35. At this same pressure ratio, the adiabatic efficiency was increased from 0.87 to 0.95. The peak efficiency at design speed was increased from 0.93 to 0.95 as a result of the rotor modification. The peak pressure ratio was decreased at all speeds as a result of the increase in outlet axial velocity. For instance, at design speed, the peak pressure ratio decreased from 1.42 to 1.40.

One of the principal effects of the rotor modification seen in figure 4 is the increase in the weight-flow operating range. At design speed, the weight-flow range was increased approximately 100 percent. The weight-flow range of both rotors was determined by the same criterion. Maximum weight flow, of course, was the maximum weight flow that could be passed before the compressor choked. From figure 4 it is apparent that at design speed the modified rotor system choked downstream of the measuring station because the over-all pressure ratio could not be reduced below a value of 1.30. Choking at the reduced weight flow for the modified rotor was caused by the reduced over-all pressure ratio and the reduced annular outlet area. The minimum weight flow for both rotor configurations was determined as the weight flow at which (1) vibrations were indicated by the plug-type vibration pickup and (2) the tip-section blade-element efficiencies (as calculated during tests) were the same for both rotors.

Rotor Inlet Conditions

The radial variation of the inlet axial velocity is presented in figure 5 for the weight-flow points near peak efficiency at corrected tip speeds of 600, 800, 1000, and 1150 feet per second. The radial variation of axial velocity is presented as a plot of the ratio of axial velocity to mean-radius axial velocity. For comparison purposes, the radial variation of axial velocity for the original rotor is included for the peak-efficiency design-speed case (fig. 5(c)). As shown in figure 5(c), the tip taper modification caused the axial velocity to decrease toward the rotor tip radius. This decrease in axial velocity can be attributed to the variation of streamline curvature caused by the addition of the insert.

For low hub-tip diameter rotors, the variation in the axial-velocity distribution at the rotor inlet is primarily a function of the curvature of the hub and tip passages. The thickness of the blades (ref. 7), however, also has an effect on the inlet axial-velocity distribution. In order to investigate the magnitude of the effect of blade thickness on the axial-velocity distribution at the rotor inlet, the axial-velocity distribution was determined experimentally by replacing the rotor with a dummy hub section (blades removed) and drawing air through the unit. The axial-velocity distributions thus obtained for both the original and modified rotor configurations are presented in figure 6. Again, as shown in figure 5, the variation of the streamline curvature caused by the addition of the insert on the modified rotor configuration caused the axial-velocity distribution to decrease toward the rotor tip radius. In comparing figures 5(c) and 6 (for both the original and modified rotor configurations), it can be seen that the presence of the rotor blades decreased the axial velocity toward the hub radius. At the hub section (10 percent of the passage height from the hub), the

presence of the blades decreased the axial velocity approximately 4 percent. This decrease in axial velocity toward the hub section is the result of blades blocking more of the passage area at that section and forcing the flow up radially.

The radial variation of the relative inlet air angles for the modified rotor are presented in figure 7 for the weight-flow points near peak efficiency at corrected tip speeds of 600, 800, 1000, and 1150 feet per second. The design relative inlet air angles and the design blade inlet angles are included in figure 7(c) for the design-speed case. The difference between the design and actual relative inlet air angles can be attributed to the deviation from the design weight flow and the design axial-velocity distribution. As pointed out in reference 2, the rotor was designed for a weight flow of 34.9 pounds per second per square foot of frontal area with constant inlet axial velocity assumed along the radius.

Rotor Outlet Conditions

As in the case for the rotor inlet, the axial-velocity distribution after the rotor was experimentally determined with the dummy hub section (blades removed) and with air drawn through the rotor. The axial-velocity distributions thus obtained are presented in figure 8 for both the original and modified rotor configurations. The effect of hub curvature in the original rotor configuration (constant tip diameter) is an increase in the axial velocity toward the hub radius. This is the result of the static-pressure gradient (high static pressure at the tip, low at the hub) which is imposed by the hub curvature. The addition of tip curvature in the modified rotor configuration reduces the effect of hub curvature and increases the axial velocity toward the tip radius.

Although the results of figure 8 were obtained with the dummy hub section, the axial-velocity distributions thus obtained after the rotor are indicative of those for ideal free-vortex flow through a rotor. This is true since, for ideal vortex flow through a rotor (zero gradients of stagnation temperature and entropy), the variation of axial velocity after the blade row is determined entirely by the curvature of the inner and outer walls (effect of blade thickness neglected).

Since true vortex flow is not achieved through a rotor, it is not surprising that the actual axial-velocity distributions after the rotor (fig. 9) do not coincide with the axial-velocity distributions for the free-vortex case (blades removed) (fig. 8). Figure 9 is a plot of the axial-velocity distribution after the rotor for the original and modified rotors at a flow near the peak-efficiency point at design speed. The velocity distribution after the modified rotor (fig. 9) appears to be very similar to the velocity distribution measured in the flow test

of the modified annular passage (fig. 8). The axial-velocity distribution of the original rotor (fig. 9), however, varies somewhat from the velocity distribution measured in the flow tests of the original annular passage. It is apparent that, for the original configuration, the radial gradient of axial velocity is much greater with the blades installed (fig. 9) than with the blades removed (fig. 8). The low axial velocity near the tip is the result of the large loss (large entropy gradient) that was indicated near the tip of the original rotor (ref. 2).

Blade-Element Performance At Design Speed

Radial distribution of blade-element efficiency. - The radial distribution of blade-element efficiency for the original and modified rotors is presented in figure 10 as a function of the percentage of passage height. The data are presented for the weight flow near the rotor over-all peak-efficiency point at design speed for each rotor. As shown by the figure, there is little change in the blade-element efficiency over the blade except near the tip section (10 percent of passage height from the outer wall). At the tip section the modified rotor increased the blade-element efficiency approximately 15 points for the given flow condition. In order to analyze the cause of the increased efficiency at the rotor tip section, a detailed comparison of the blade-element performance characteristics at the tip section for the original and modified rotors will be presented in the following section.

Tip-section blade-element performance characteristics. - The rotor-blade tip-element performance characteristics (deviation angle, total-pressure-loss coefficient, relative inlet Mach number, diffusion factor, axial-velocity ratio, efficiency, work coefficient, and total-pressure ratio) for the original and modified rotors at design speed are compared in figure 11 as a function of incidence angle. Included in figure 11 are plots of specific weight flow which have been included to facilitate the task of locating a blade-element performance point on the over-all performance map (fig. 4). As previously discussed, the blade geometry for the two rotor tip sections are not exactly equivalent because of the shift in flow across the blade. The effect of this geometry difference is believed to be extremely small as compared with the difference in aerodynamic parameters.

Since the inlet radius to both tip sections was identical and there was only a slight change in the inlet blade angle, the relative inlet Mach number for a given incidence angle (fig. 11) remained essentially constant (approximately 1.0 at design speed).

The rotor modification increased the axial-velocity ratio across the rotor tip section from approximately 0.94 to 1.24 at the near-minimum-loss incidence angle of 4.5°. This large increase in axial-velocity ratio across the modified tip section can be attributed to

(1) the increase in blade-element efficiency (the reduced entropy gradient) and (2) the thickness and curvature of the insert.

At an incidence angle of 4.5° (approximate minimum-loss incidence angle), the rotor modification decreased the diffusion factor at the tip section from 0.45 to 0.30. The total-pressure-loss coefficient was decreased from 0.14 to 0.04, and the corresponding adiabatic efficiency increased from 0.80 to 0.92. For a given diffusion-factor value near the minimum-loss incidence angle, the rotor modification reduced the total-pressure-loss coefficient even though the incidence angle was increased. For example, at a diffusion factor of 0.4, the rotor modification decreased the total-pressure-loss coefficient from 0.14 to 0.075 even though the incidence angle was increased from 4° to 6°. It is interesting to note that maximum incidence angle (fig. 11), as determined by the vibration pickup plug and the tip blade-element efficiency, occurred approximately at the same value of diffusion factor for the original and modified rotors. It should be pointed out, however, that the minimum incidence angle for the modified rotor was determined by the flow limitations of the rig. As pointed out previously in the section Over-All Performance, the modified rotor configuration choked downstream of the measuring station, and it was not possible to obtain the absolute minimum value of incidence angle.

Although the camber angle of the modified tip section was greater than that of the original rotor, the total-pressure ratio and the dimensionless work coefficients at an incidence angle of 4.5° decreased from 1.38 to 1.33 and from 0.38 to 0.29, respectively. The increased turning at the tip section for the modified rotor tended to increase the blade-outlet tangential velocity and therefore the work input and total-pressure ratio; however, the increased axial-velocity ratio overcompensated this effect and actually decreased the work input and total-pressure ratio across the blade section.

The decrease in deviation angle at optimum incidence angle is assumed to be caused by either the increase in axial-velocity ratio or the decrease in the total-pressure-loss coefficient. In accordance with Carter's rule (ref. 8), the deviation angle for the modified tip section should have been approximately 0.5° greater than the deviation angle for the original tip section because of the slight camber difference.

The variation of the rotor-blade tip-section total-pressure-loss coefficient at the near-minimum-loss incidence angle with inlet relative Mach number is presented in figure 12 for the original and modified rotor at tip speeds of 600, 800, 1000, and 1050 feet per second and 1150 feet per second for the modified rotor. For higher values of relative inlet Mach number, the modified-rotor loss coefficient is less than that of the original rotor. For example, at an inlet Mach number of 1.05 the rotor modification decreased the loss coefficient from

0.125 to 0.05. These results show that the decreased loss obtained with the rotor modification of the higher wheel speeds is a result of the blade loading rather than the inlet relative Mach number.

Although the two-dimensional diffusion factor is used as a blade-loading parameter, it may not be a general blade-loading criterion in actual three-dimensional flow. The magnitude of the loss coefficient affects the velocity ratio across the rotor, which, in turn, influences the magnitude of the diffusion factor at the blade element. In addition, the velocity ratio influences the boundary-layer characteristics along the annulus walls, which may, in turn, influence the blade-element characteristics. In general, the three-dimensional character of the flow makes the two-dimensional evaluated diffusion factor only an approximate blade-loading parameter.

Outlet boundary-layer blockage factor. - The outlet boundary-layer blockage factor is defined as the ratio of the ideal to the actual weight flow along the radius at the rotor outlet measuring station. Actual weight flow is determined by integrating a curve of weight flow against radius; ideal weight flow is determined by extrapolating the general contour shape of the actual weight-flow curve through the boundary-layer regions to the walls and integrating the resultant curve. Curves of actual and ideal weight flows against radius are presented in figure 13 for both the original and modified rotors for the near overall peak-efficiency weight-flow points at design speed. The shaded areas of figure 13 represent the difference between the actual and ideal weight flows. The shaded area for the modified rotor (fig. 13) is smaller than the shaded area for the original rotor and represents a decrease in the boundary-layer blockage factor from approximately 3 to $1\frac{1}{2}$ percent.

MODIFIED-ROTOR-BLADE-ELEMENT PERFORMANCE

The blade-element performance characteristics of the modified rotor tip section at design speed are presented in figure 11 together with the blade-element performance characteristics of the original rotor tip section. In figure 14, the blade-element performance characteristics of the modified rotor are presented for all five of the major radial measuring stations (10, 30, 50, 70, and 90 percent of the passage height from hub to tip) for the corrected tip speeds of 600, 800, 1000, 1050, and 1150 feet per second. The extensive data are presented to further supplement the published data on transonic rotor-blade performance. In general, except for the rotor tip section, the trend of the various blade-element performance characteristics with incidence angle are consistent with the trends observed for the original rotor (ref. 2). Therefore, only an abbreviated discussion of the modified-blade-element performance will be included.

As previously experienced, the minimum total-pressure-loss coefficient at the rotor tip section (fig. 14(a)) increased and shifted to higher values of incidence angle as the speed or relative inlet Mach number was increased. Although it would have been desirable to determine the loss - incidence angle relation of lower incidence angles for higher speeds, the test-rig flow-area limitations prevented operation in this region.

Some of the blade-element characteristics at a corrected tip speed of 1150 feet per second did not vary consistently with the corresponding blade-element characteristics at the lower tip speeds and were omitted in figure 14. The deviation angle, for instance, increased sharply for all radial positions. The axial-velocity ratio across the rotor (near optimum incidence angle) increased rather than decreased as the tip speed was increased from 1050 to 1150 feet per second. Also, the diffusion factor decreased pronouncedly as the tip speed was increased from 1050 to 1150 feet per second. A thorough examination of the data at a tip speed of 1150 feet per second indicated that an error was made in measuring the absolute outlet angle after the rotor. This error is attributed to the angle measuring instrument not being correctly alined with the compressor axis during the test run at 1150 feet per second. For example, an increase of approximately $4\frac{1}{2}^{\circ}$ in the measured outlet angle would decrease the deviation angle approximately 2° at the tip and 4° at the hub. A decrease in deviation angle would decrease the axial-velocity ratio across the rotor and increase the diffusion factor. Calculation showed that an error of approximately $4\frac{1}{2}^{\circ}$ in the measured outlet angle would make the data (deviation angle, axial-velocity ratio, and diffusion factor) consistent with the data measured at the other speeds. A check of the integrated weight flows after the rotor also indicated better agreement when the absolute rotor outlet angle was increased. The remaining blade-element characteristics (relative inlet Mach number, efficiency, total-pressure ratio, total-pressure-loss coefficient, and dimensionless work coefficient) would not change since they are measured independently and are not a function of the measured outlet angle. For this reason the 115-percent data, which are a function of the measured outlet angle, were omitted in figure 14.

SUMMARY OF RESULTS

The 0.4 hub-tip diameter ratio transonic rotor was modified by introducing tip curvature to reduce the rotor tip-section blade loading. In comparison with the performance of the original rotor configuration, the following results were obtained:

1. At design corrected tip speeds of 1000 feet per second, the rotor modification increased the over-all peak efficiency from 0.93 to

[redacted]

0.95 and decreased the maximum pressure ratio from 1.42 to 1.40. The rotor modification also had a larger useful weight-flow range at design speed. At 115 percent design speed, the over-all-performance peak efficiency for the rotor modification was 0.92.

2. Tip curvature across a rotor-blade row had a pronounced effect on the axial-velocity distribution before and after the rotor and may be a useful design tool in controlling blade-element loading. For the given tip contour, the axial velocity decreased toward the tip at the rotor inlet and increased toward the tip at the rotor outlet. The effect of these velocity changes was a marked reduction in tip loading.

3. At design speed, the rotor modification increased the tip-section blade-element peak efficiency from 0.80 to 0.92. The rotor modification also decreased the diffusion factor from 0.45 to 0.30 and increased the axial-velocity ratio from 0.94 to 1.24 at the tip section for the near-minimum-loss incidence angle of 4.5°.

4. For a given diffusion-factor value of 0.40, the rotor modification decreased the total-pressure-loss coefficient at the tip section from 0.14 to 0.075. This value of diffusion factor was obtained in the modified rotor at an incidence angle appreciably greater than the minimum-loss value.

5. Comparison of the performance of the modified rotor with the performance of the original rotor indicated that the decrease in tip efficiency with increase in speed that was noted in the tests of the original rotor was the result of the increased blade loading rather than the increased inlet relative Mach number.

Lewis Flight Propulsion Laboratory
National Advisory Committee for Aeronautics
Cleveland, Ohio, December 7, 1955

[redacted]

APPENDIX A

SYMBOLS

The following symbols are used in this report:

A,B,C,D,E,	blade radial measuring stations
A_f	compressor frontal area, sq ft
c_p	specific heat of air at constant pressure, Btu/(lb)($^\circ$R)
D	diffusion factor
g	acceleration due to gravity, 32.17 ft/sec^2
H	total enthalpy, ft-lb/lb
i	angle of incidence, angle between tangent to blade mean camber line at leading edge and inlet-air direction, deg
J	mechanical equivalent of heat, 778 ft-lb/Btu
M	Mach number
n	summation value
P	total pressure, lb/sq ft
r	radius, in.
T	total temperature, $^\circ$R
U	blade speed, ft/sec
V	velocity of air, ft/sec
W	weight flow, lb/sec
β	angle between velocity vector and rotor axis, deg
γ	ratio of specific heats
δ	ratio of inlet pressure to standard NACA sea-level pressure, P/2116.2

δ°	deviation angle, angle between tangent to mean camber line at blade trailing edge and air direction, deg
η	adiabatic efficiency
θ	ratio of inlet total temperature to standard NACA sea-level temperature, T/518.6
ρ	static air density, slugs/cu ft
σ	solidity ratio, ratio of blade chord to blade spacing
φ	blade-camber angle, deg
π	blade inlet angle, angle between tangent to blade mean line and rotor axis at blade leading edge, deg
ω	total-pressure-loss coefficient

Subscripts:

i	ideal
m	mean radius
R	rotor
t	tip section
z	axial direction
θ	tangential direction
1	rotor inlet
2	rotor outlet

Superscript:

'	relative to rotor

[redacted]

APPENDIX B

EQUATIONS

The equations used for the blade-element and over-all performance are included below.

Over-All Performance

The over-all arithmetic-averaged adiabatic efficiency for the rotor is

$$\eta = T_1 \sum_{n=1}^{n} \frac{1}{n} \left[\frac{\left(\frac{P_2}{P_1}\right)^{\frac{\gamma-1}{\gamma}} - 1}{T_2 - T_1} \right] \tag{1}$$

The over-all arithmetic-averaged total-pressure ratio is

$$\frac{P_2}{P_1} = \sum_{n=1}^{n} \frac{1}{n} \frac{P_2}{P_1} \tag{2}$$

Rotor-Blade Element

The equation for the rotor-blade-element relative total-pressure coefficient (ref. 3) is

$$\omega = \left(\frac{P_2'}{P_1'}\right)_i \left[\frac{1 - \left(\frac{P_2}{P_1}\right)\left(\frac{T_1}{T_2}\right)^{\frac{\gamma}{\gamma-1}}}{1 - \left(1 + \frac{\gamma-1}{2} M_1'^2\right)^{-\frac{\gamma}{\gamma-1}}} \right] \tag{3}$$

where $\left(\frac{P_2'}{P_1'}\right)_i = \left\{ 1 + \frac{\gamma-1}{2} M_R'^2 \left[1 - \left(\frac{r_1}{r_2}\right)^2 \right] \right\}^{\frac{\gamma}{\gamma-1}} \approx 1$ for a given rotor design and M_R is the wheel rotational Mach number (outlet wheel tangential velocity divided by inlet relative stagnation velocity of sound).

[redacted]

The blade-element adiabatic efficiency is

$$\eta = \frac{T_1\left[\left(\frac{P_2}{P_1}\right)^{\frac{\gamma-1}{\gamma}} - 1\right]}{T_2 - T_1} \tag{4}$$

In terms of ω, M_1', and T_2/T_1, the blade-element adiabatic efficiency (ref. 4) is for $(P_2'/P_1)_i = 1.0$

$$\eta = \frac{\frac{T_2}{T_1}\left\{1.0 - \omega\left[1.0 - \left(1.0 + \frac{\gamma - 1}{2} M_1'^2\right)^{-\frac{\gamma}{\gamma-1}}\right]\right\}^{\frac{\gamma-1}{\gamma}} - 1.0}{\left(\frac{T_2}{T_1} - 1.0\right)}$$

The following is the equation for the dimensionless work coefficient (ref. 4):

$$\frac{\Delta H}{U_t^2} = \frac{Jgc_pT_{standard}\left(\frac{T_2}{T_1} - 1\right)}{\left(\frac{U_t}{\sqrt{\theta}}\right)^2} \tag{5}$$

The diffusion factor (ref. 3) is

$$D = \left(1 - \frac{V_2'}{V_1'}\right) + \frac{V_{\theta,1}' - V_{\theta,2}'}{2V_1'\sigma} \tag{6}$$

REFERENCES

1. Serovy, George K., Robbins, William H., and Glaser, Frederick W.: Experimental Investigation of a 0.4 Hub-Tip Diameter Ratio Axial-Flow Compressor Inlet Stage at Transonic Inlet Relative Mach Numbers. I - Rotor Design and Over-All Performance at Tip Speeds from 60 to 100 Percent of Design. NACA RM E53I11, 1953.

2. Montgomery, John C., and Glaser, Frederick W.: Experimental Investigation of a 0.4 Hub-Tip Diameter Ratio Axial-Flow Compressor Inlet Stage at Transonic Inlet Relative Mach Numbers. II - Stage and Blade-Element Performance. NACA RM E54I29, 1955.

3. Lieblein, Seymour, Schwenk, Francis C., and Broderick, Robert L.: Diffusion Factor for Estimating Losses and Limiting Blade Loadings in Axial-Flow-Compressor Blade Elements. NACA RM E53D01, 1953.

4. Schwenk, Francis C., Lieblein, Seymour, and Lewis, George W., Jr.: Experimental Investigation of an Axial-Flow Compressor Inlet Stage Operating at Transonic Relative Inlet Mach Numbers. III - Blade-Row Performance of Stage with Transonic Rotor and Subsonic Stator at Corrected Tip Speeds of 800 and 1000 Feet Per Second. NACA RM E53G17, 1953.

5. Robbins, William H., and Glaser, Frederick W.: Investigation of an Axial-Flow-Compressor Rotor with Circular-Arc Blades Operating up to a Rotor-Inlet Relative Mach Number of 1.22. NACA RM E53D24, 1953.

6. Schwenk, Francis C., and Lewis, George W., Jr.: Experimental Investigation of a Transonic Axial-Flow-Compressor Rotor with Double-Circular-Arc Airfoil Blade Sections. III - Comparison of Blade-Element Performance with Three Levels of Solidity. NACA RM E55F01, 1955.

7. Stanitz, John D.: Effect of Blade-Thickness Taper on Axial-Velocity Distribution at the Leading Edge of an Entrance Rotor-Blade Row with Axial Inlet, and the Influence of This Distribution on Alinement of the Rotor Blade for Zero Angle of Attack. NACA TN 2986, 1953.

8. Carter, A. D. S., and Hughes, Hazel P.: A Theoretical Investigation into the Effect of Profile Shape on the Performance of Aerofoils in Cascade. Power Jet Rep. No. R.1192, Res. and Dev., Power Jets, Ltd., Mar. 1946.

[redacted]

TABLE I. - COMPARISON OF ORIGINAL AND MODIFIED

ROTOR-BLADE GEOMETRY

Passage height, percent	Rotor inlet radius, r_1, in.	Rotor outlet radius, r_2, in.		Blade camber angle, Φ, deg	
		Original	Modified	Original	Modified
0 (tip)	7.00	7.00	6.75	9.4	12.6
25	5.91	6.16	6.00	14.7	17.9
50	4.82	5.33	5.24	22.5	24.7
75	3.73	4.49	4.49	30.7	32.3
100 (hub)	2.64	3.65	3.73	42.1	42.1

[redacted]

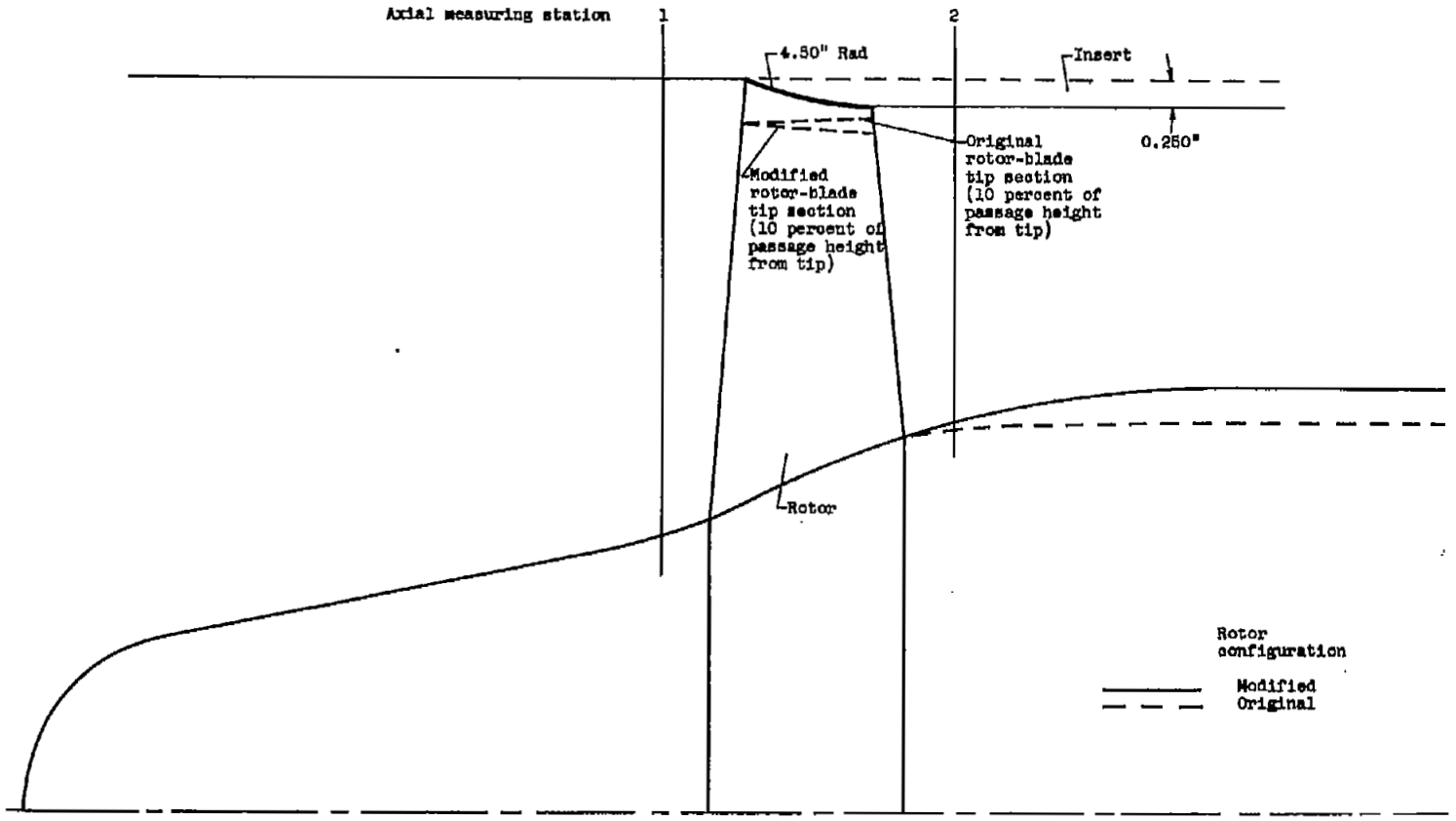

Figure 1. - Diagram of original and modified rotor configurations.

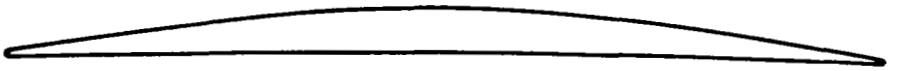

(a) Modified tip section; camber angle, 14.6°.

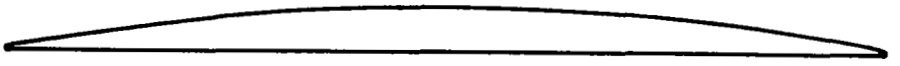

(b) Original tip section; camber angle, 11.4°.

Figure 2. - Comparison of original and modified rotor-blade tip sections along designated streamlines.

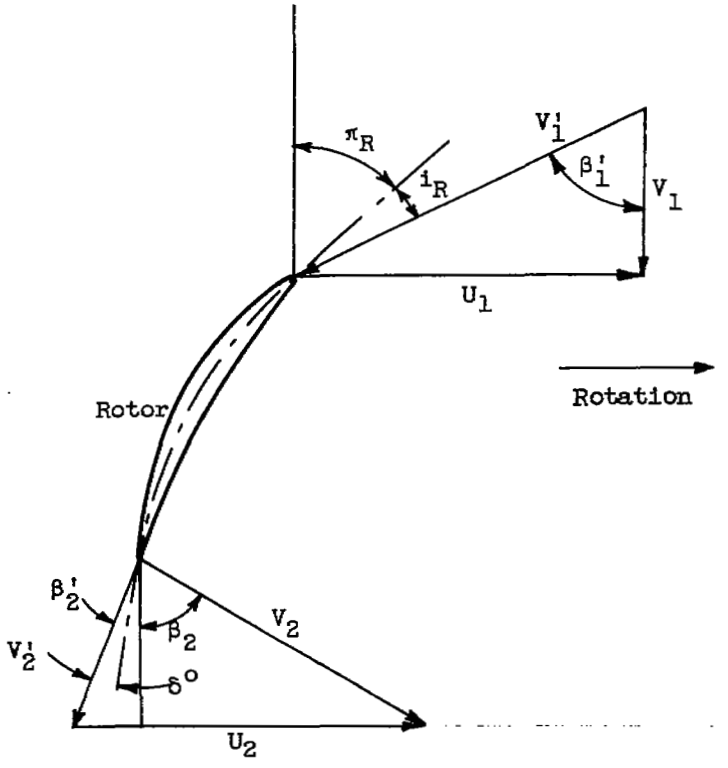

Figure 3. - Air and blade angles for a blade element.

[redacted]

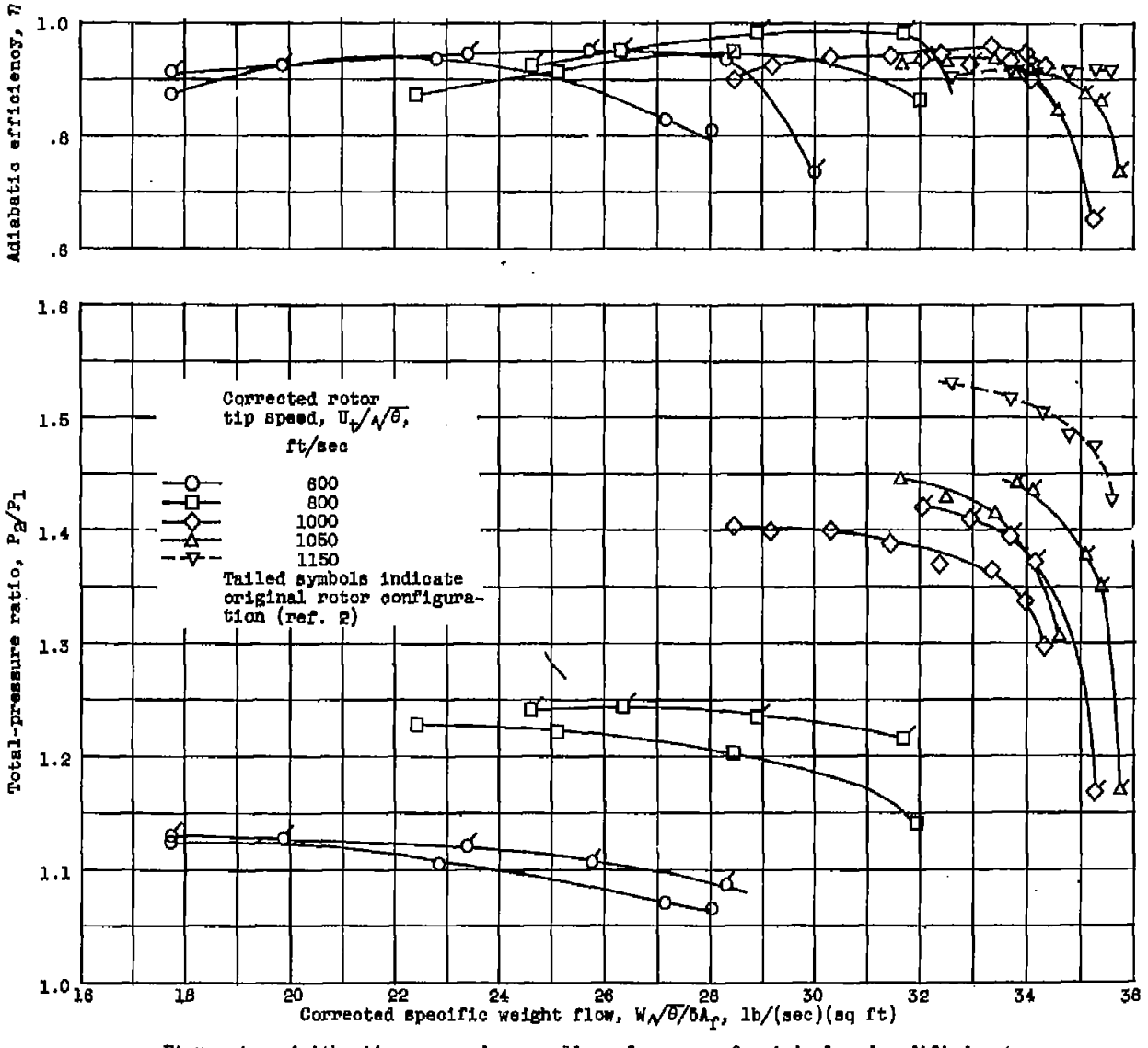

Figure 4. - Arithmetic-averaged over-all performance of original and modified rotors.

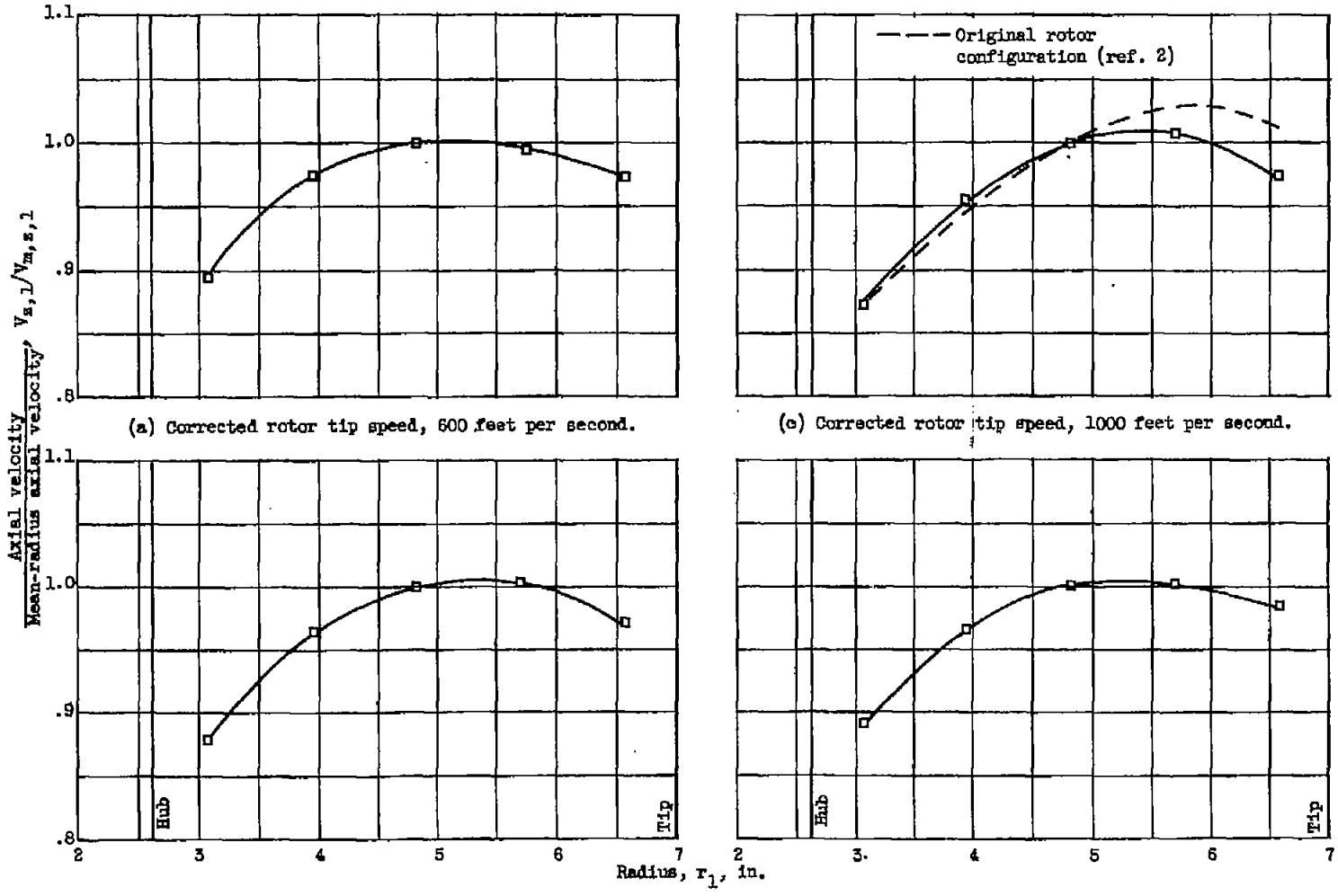

(a) Corrected rotor tip speed, 600 feet per second.

(c) Corrected rotor tip speed, 1000 feet per second.

(b) Corrected rotor tip speed, 800 feet per second.

(d) Corrected rotor tip speed, 1150 feet per second.

Figure 5. - Variation of axial velocity with radius at rotor inlet for near-peak-efficiency weight-flow points.

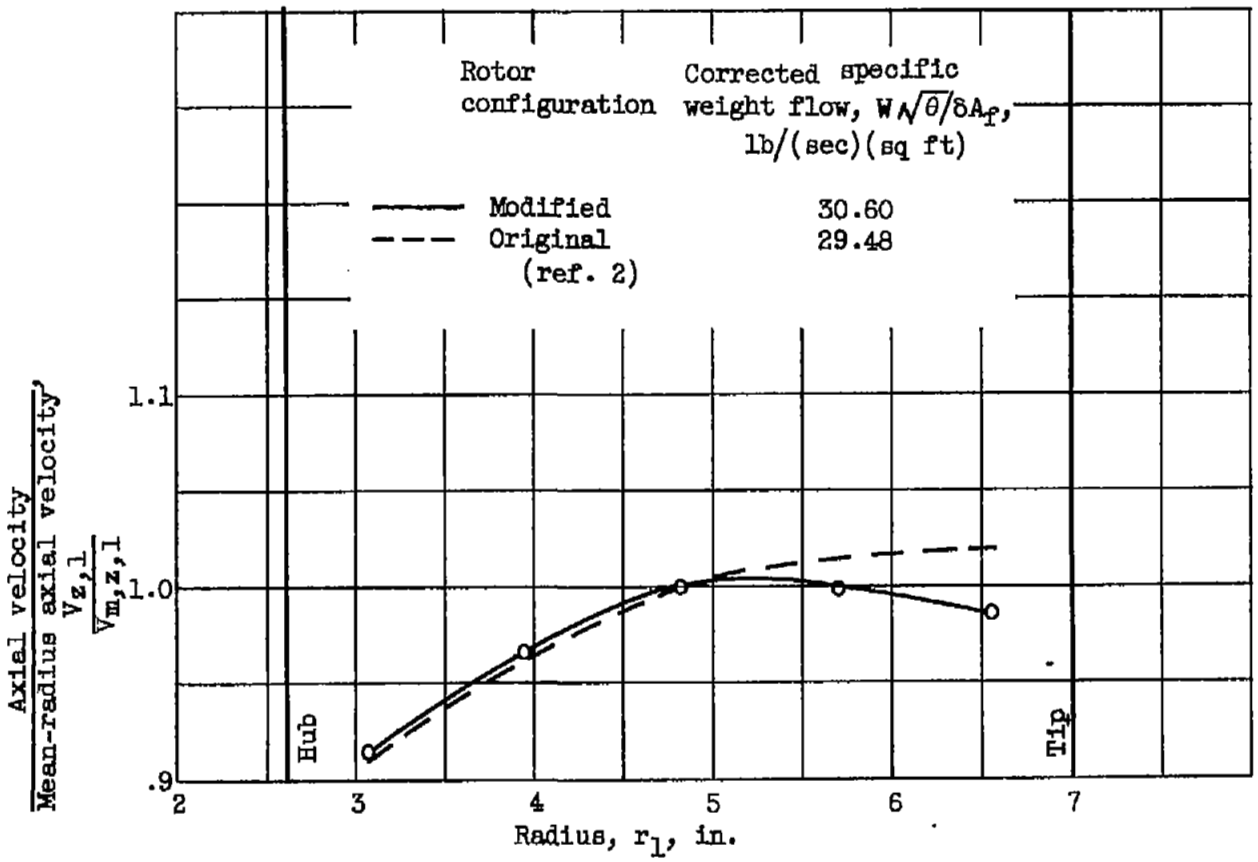

Figure 6. - Variation of axial velocity with radius at rotor inlet for original and modified rotors with rotor blades removed.

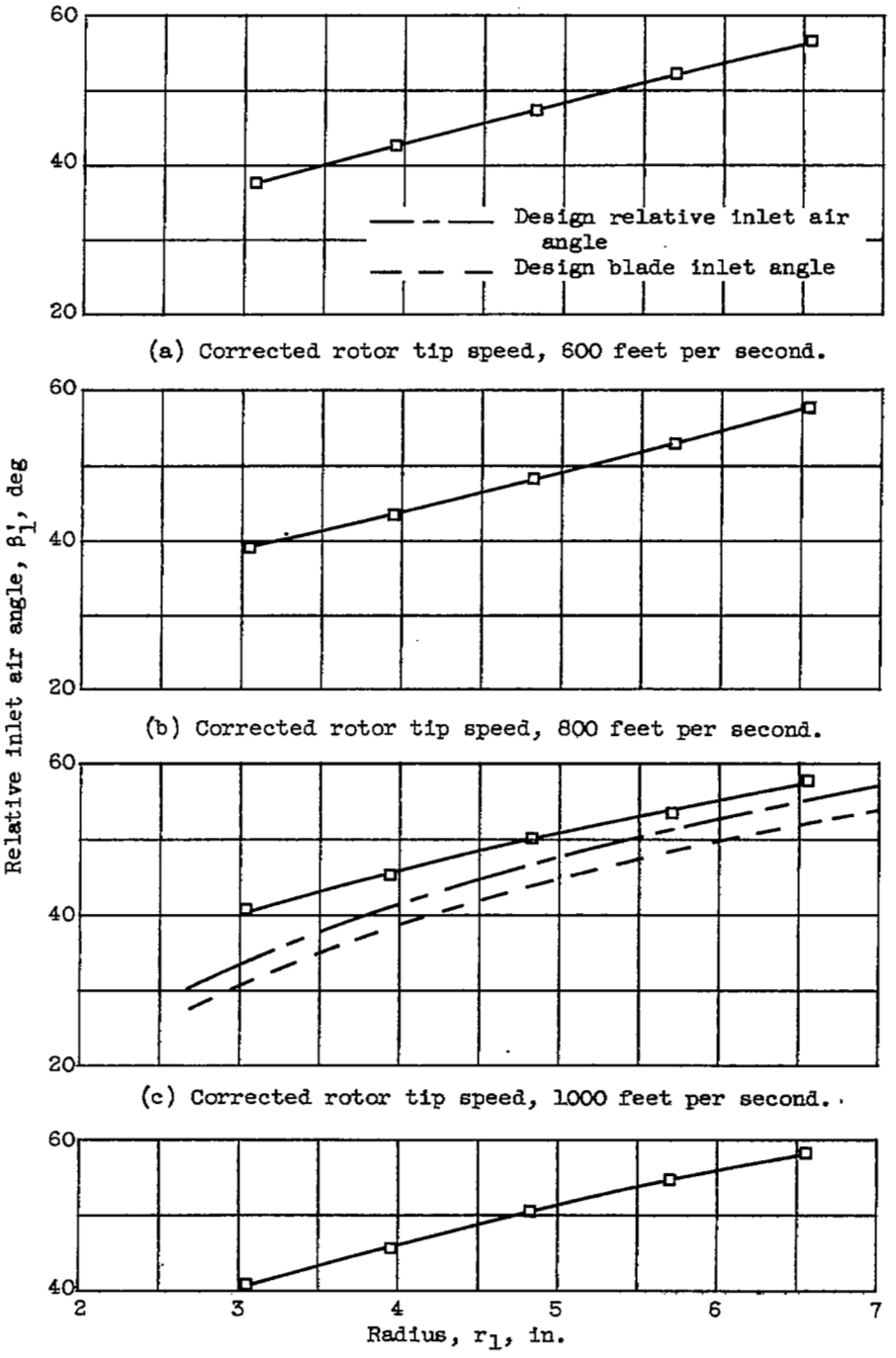

(a) Corrected rotor tip speed, 600 feet per second.

(b) Corrected rotor tip speed, 800 feet per second.

(c) Corrected rotor tip speed, 1000 feet per second.

(d) Corrected rotor tip speed, 1150 feet per second.

Figure 7. - Variation of relative inlet air angle with radius at rotor inlet for near-peak-efficiency weight-flow points.

[redacted]

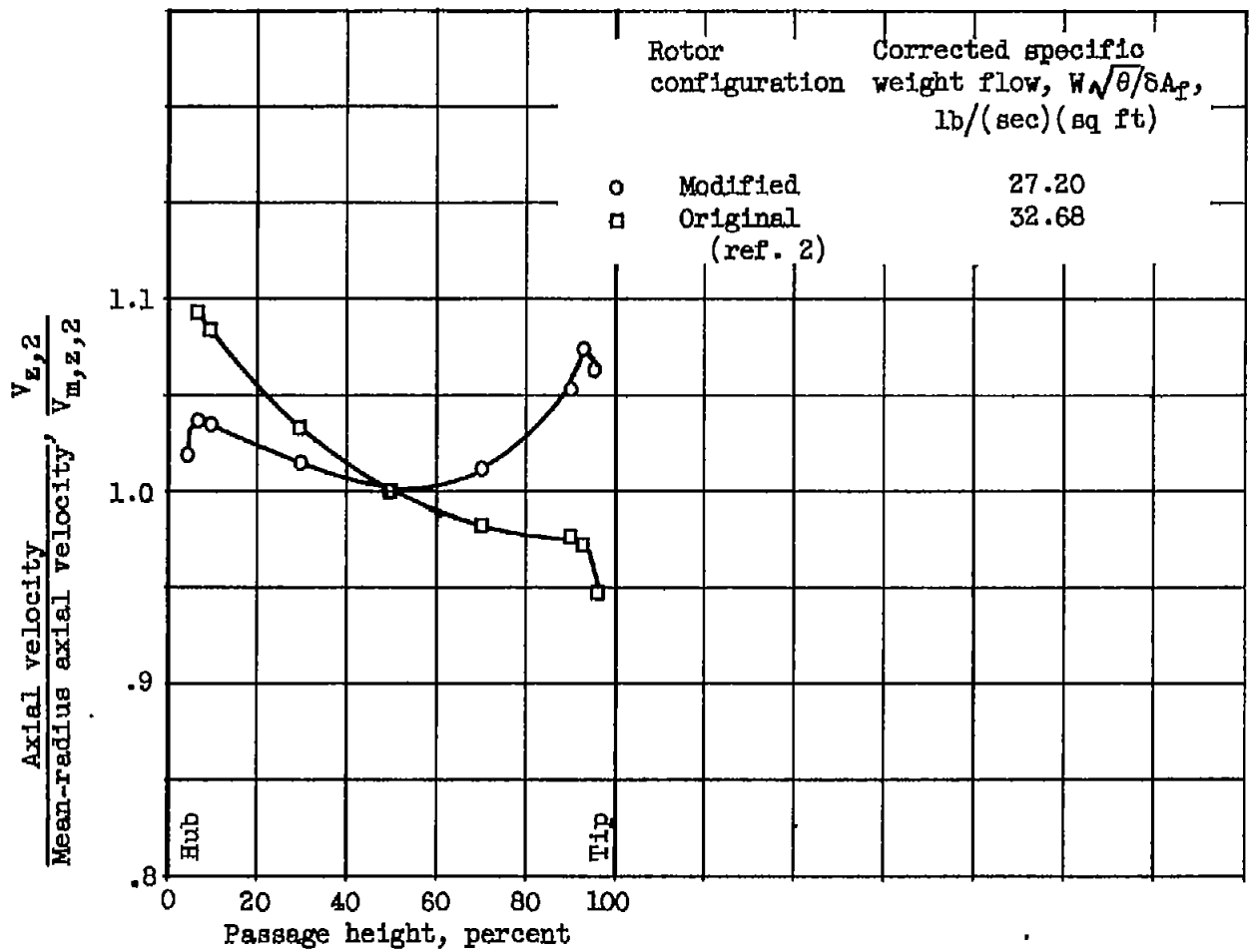

Figure 8. - Variation of axial velocity with percentage of passage height at rotor outlet for original and modified rotors with rotor blades removed.

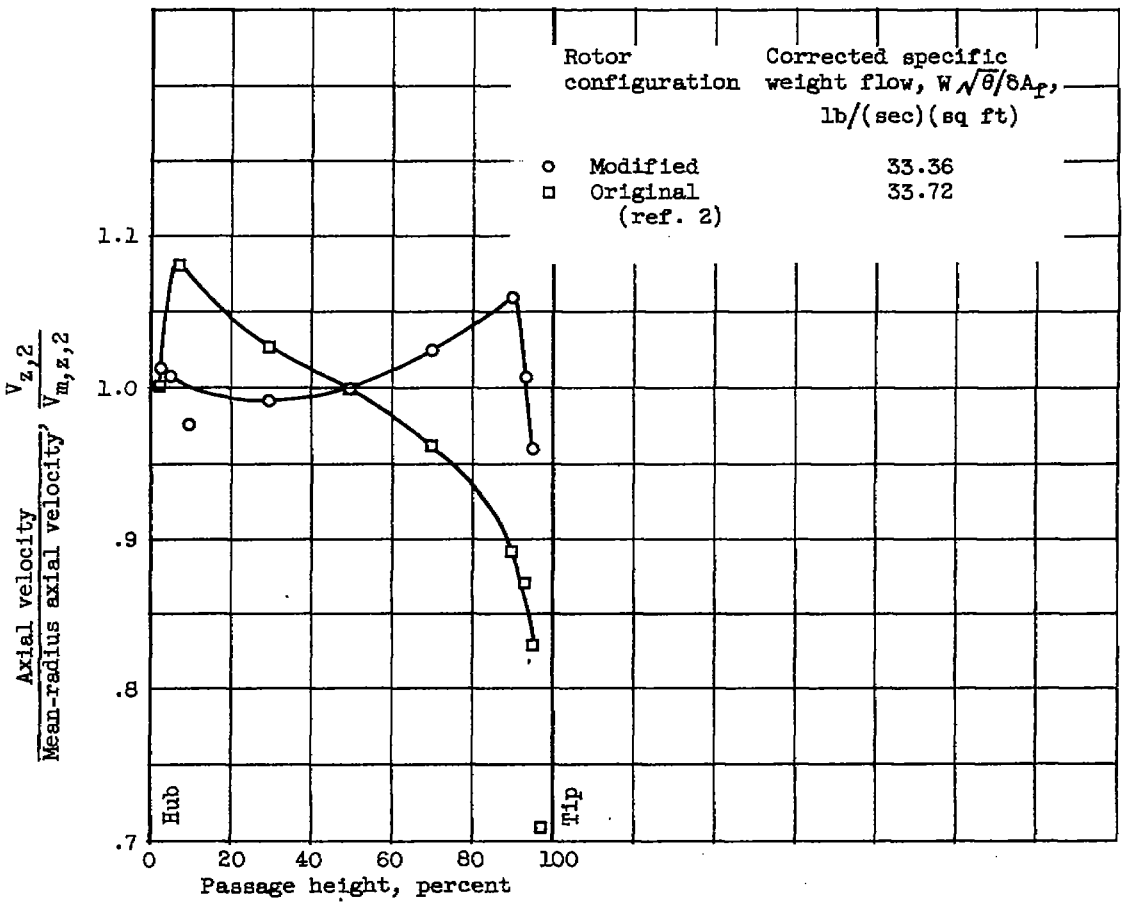

Figure 9. - Variation of outlet axial velocity with percentage of passage height for original and modified rotors. Corrected rotor tip speed, 1000 feet per second.

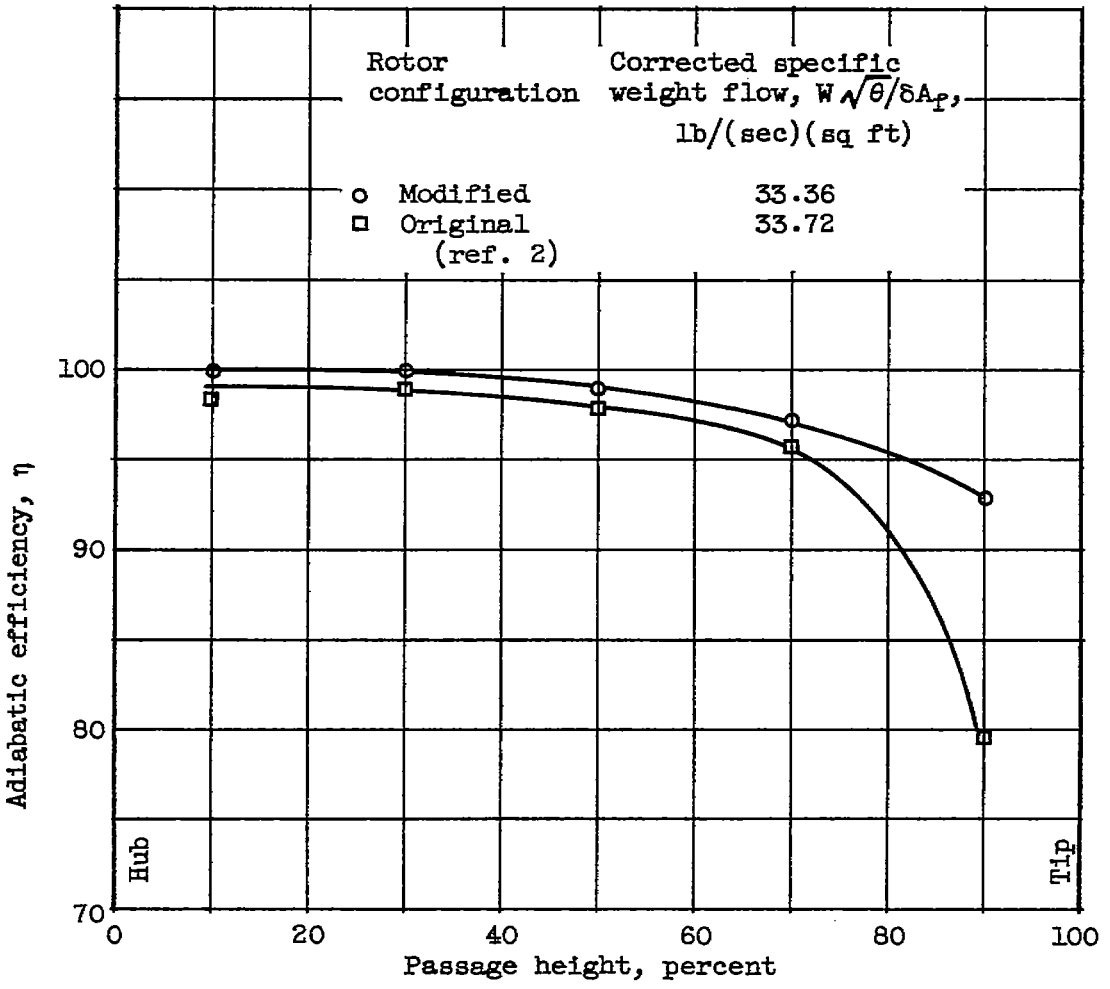

Figure 10. - Radial distribution of tip-section blade-element efficiency for original and modified rotors. Corrected tip speed, 1000 feet per second.

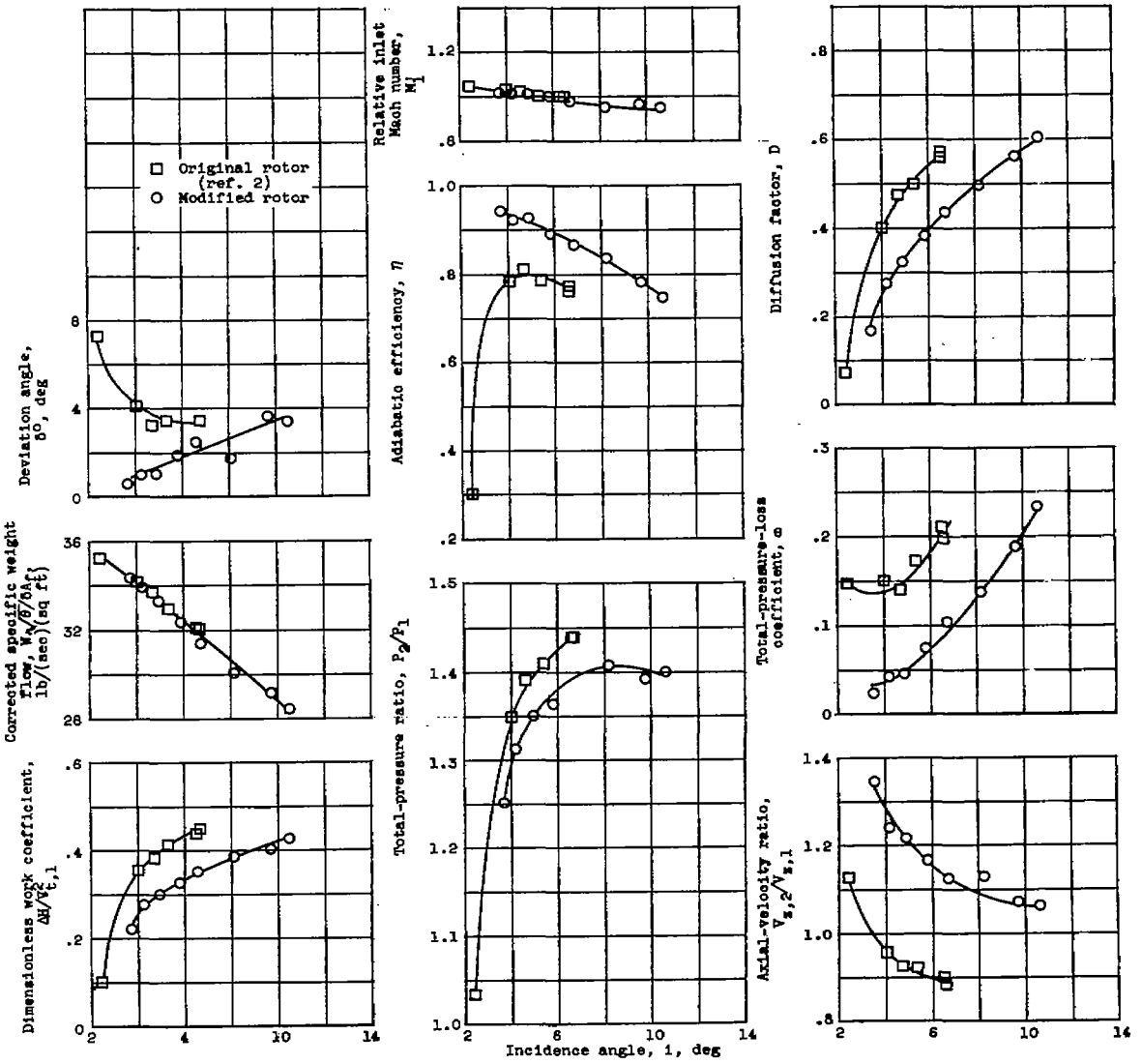

Figure 11. - Comparison of tip-section blade-element characteristics. Corrected rotor tip speed, 1000 feet per second.

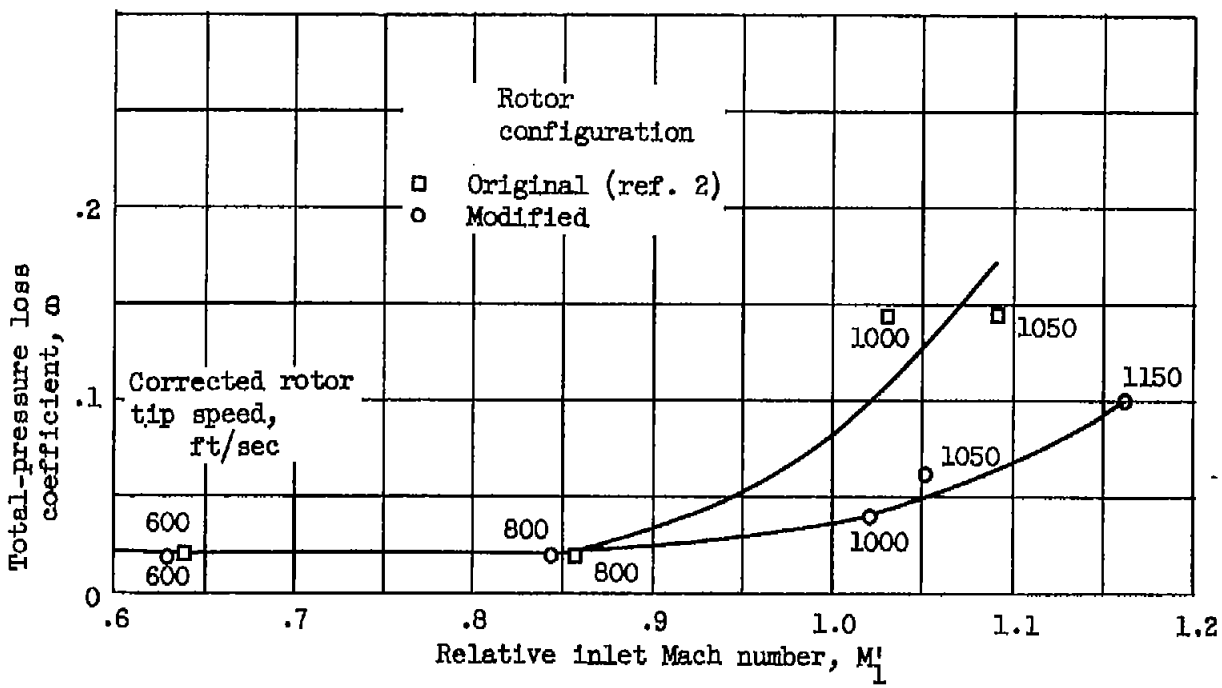

Figure 12. - Comparison of total-pressure-loss coefficient with inlet relative Mach number at near-optimum incidence angle for original- and modified-rotor tip sections.

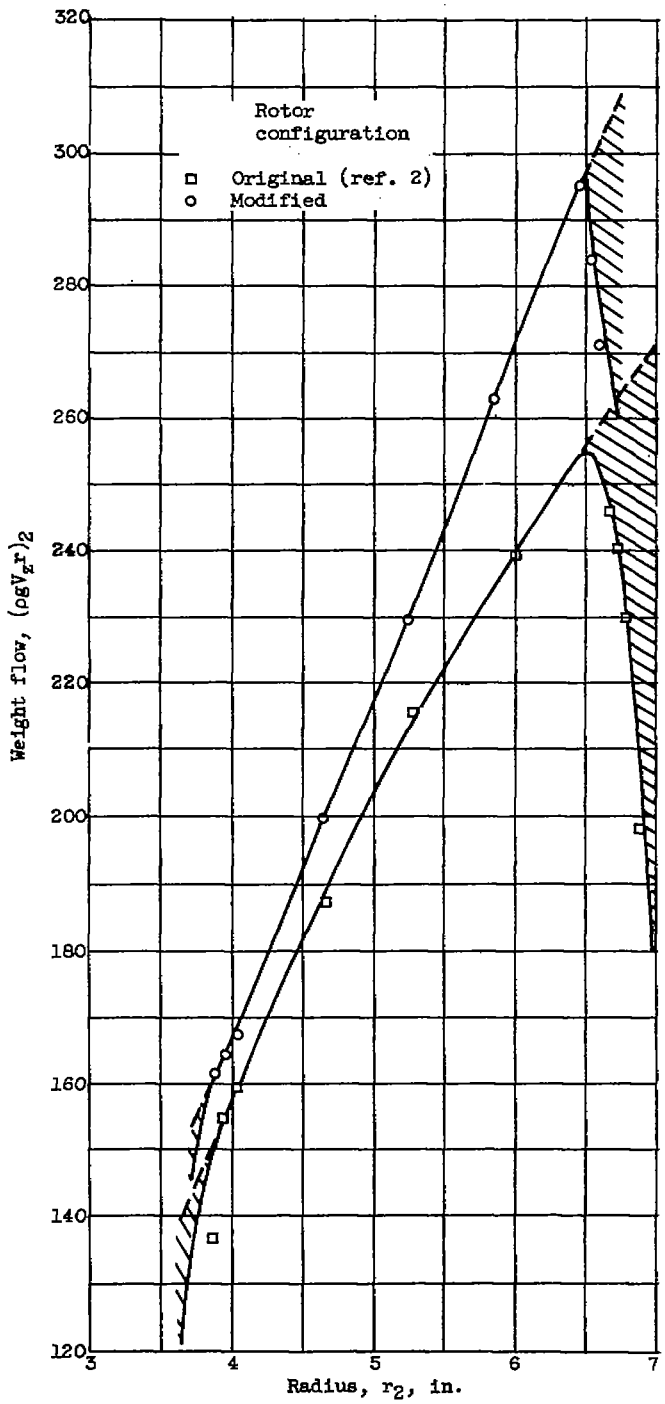

Figure 13. - Comparison of actual and ideal weight flows after the rotor at design speed and overall peak-efficiency weight-flow points for original and modified rotors.

[redacted]

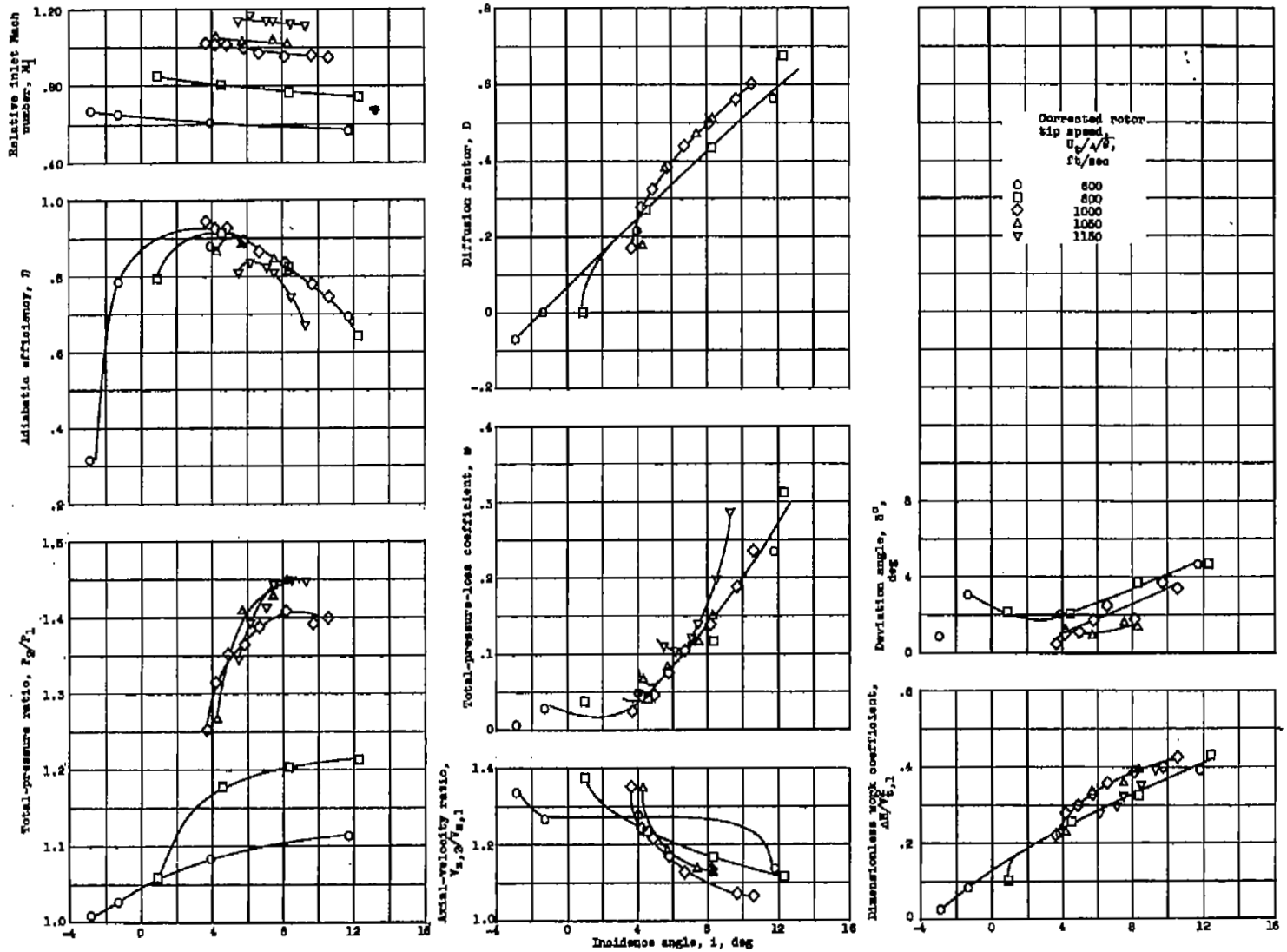

(a) Radial station A (10 percent of passage height from tip).

Figure 14. - Modified-rotor-blade-element data.

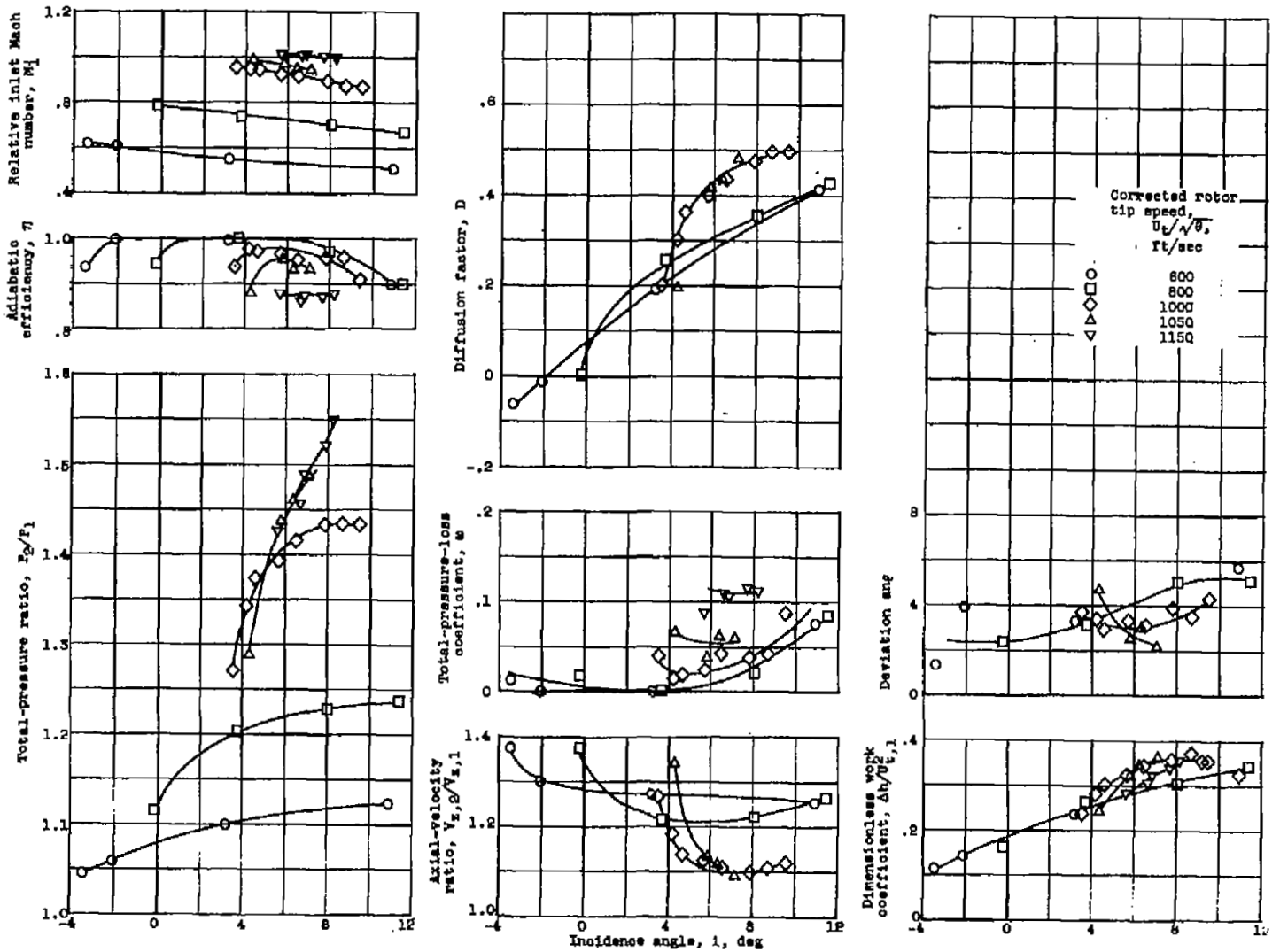

(b) Radial station B (50 percent of passage height from tip).

Figure 14. - Continued. Modified-rotor-blade-element data.

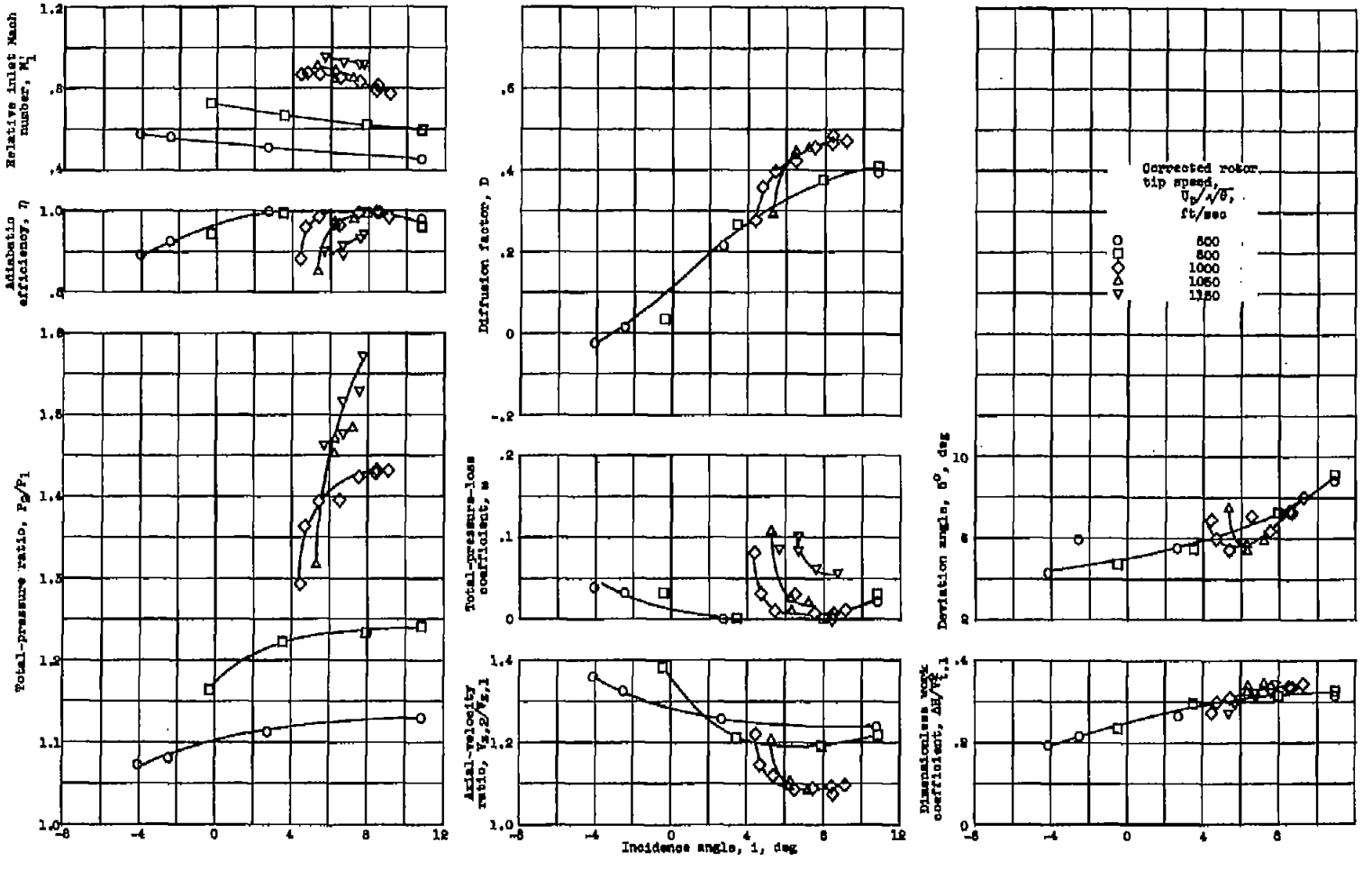

(c) Radial station C (50 percent of passage height from tip).

Figure 14. - Continued. Modified-rotor-blade-element data.

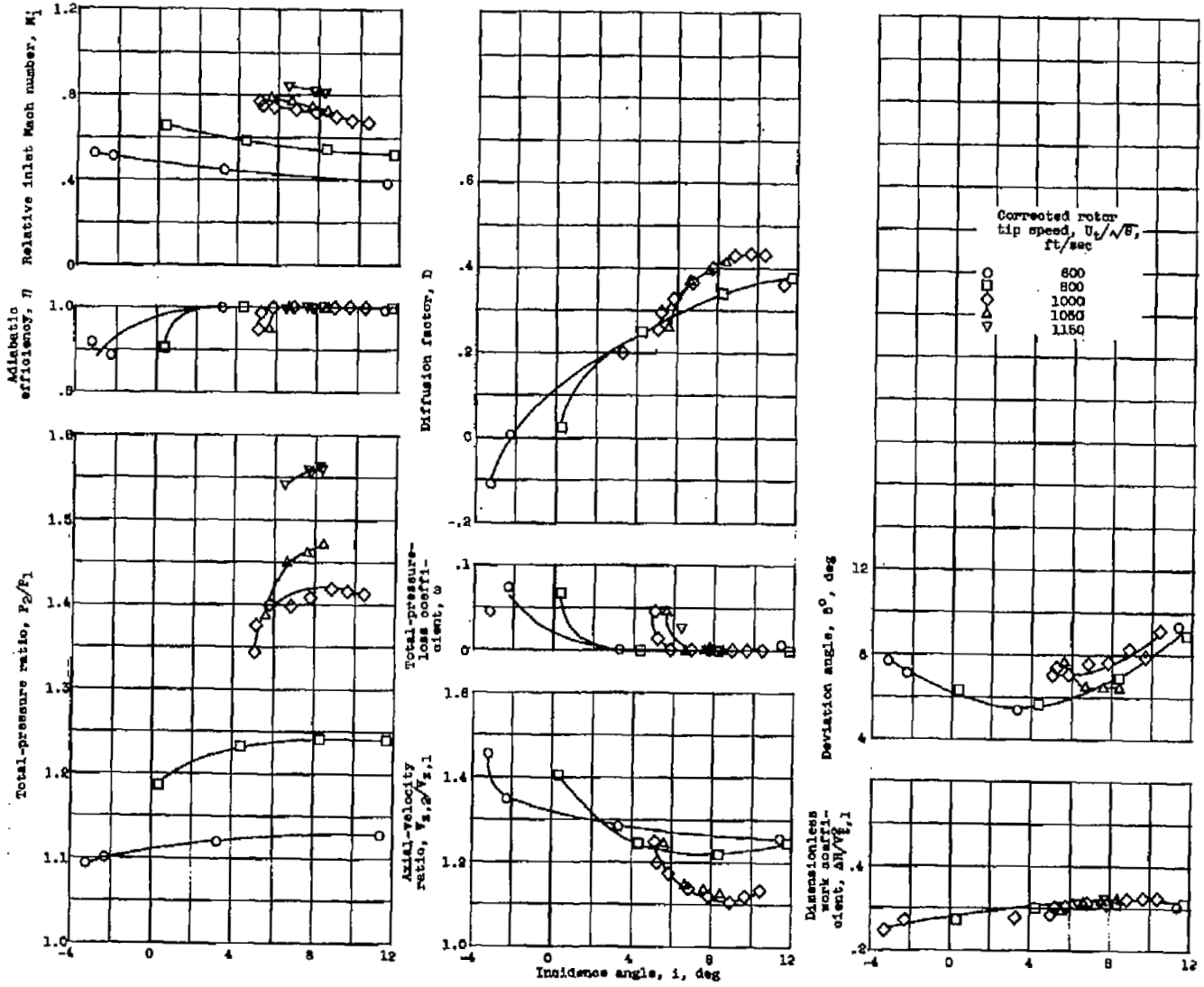

(d) Radial station D (70 percent of passage height from tip).

Figure 14. - Continued. Modified-rotor-blade-element data.

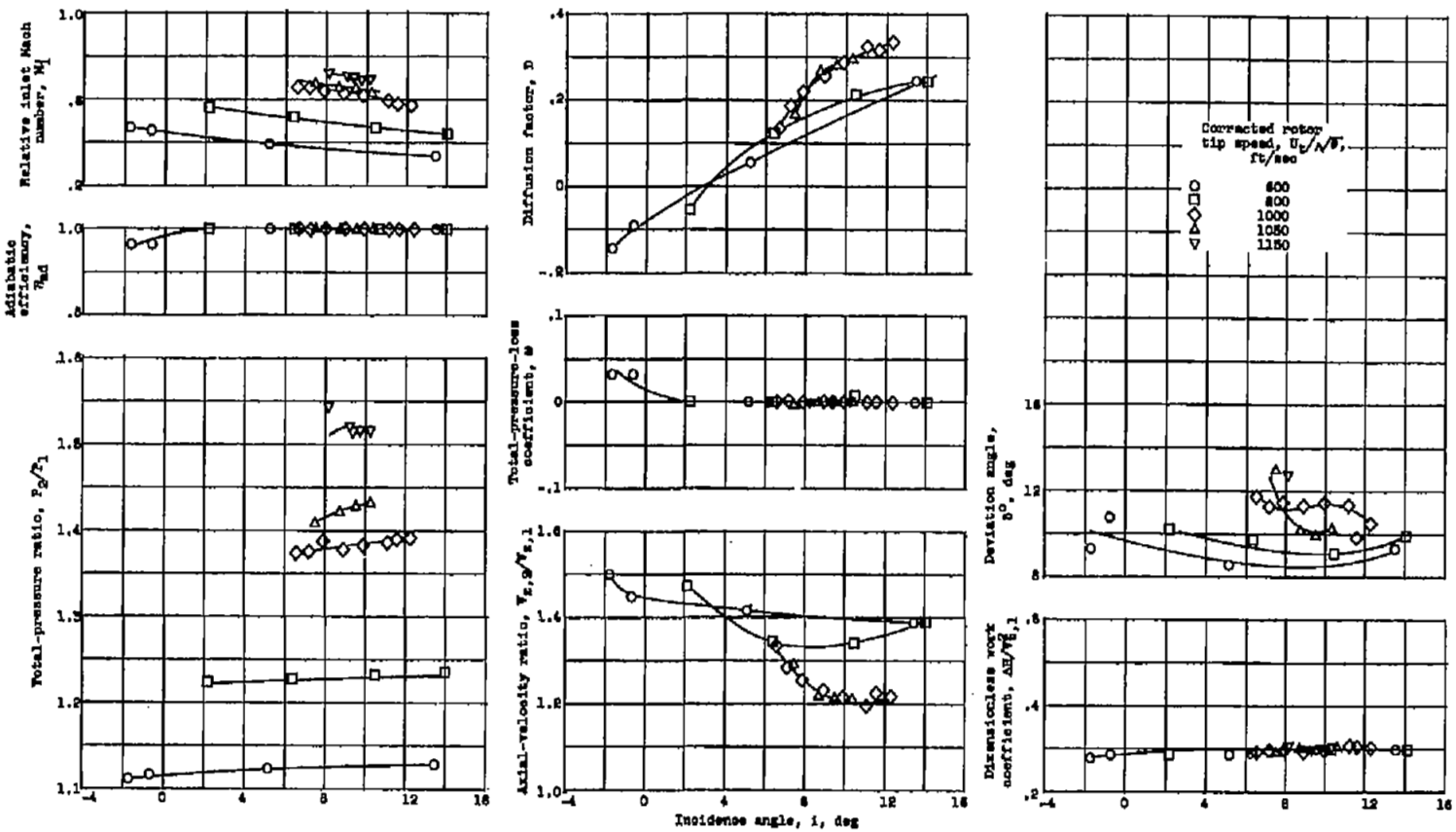

(e) Radial station E (90 percent of passage height from tip).

Figure 14. - Concluded. Modified-rotor-blade-element data.